

# A proteorhodopsin-based biohybrid light-powering pH sensor†

Cite this: *Phys. Chem. Chem. Phys.*, 2013, **15**, 15821

Received 20th July 2013,  
Accepted 2nd August 2013

DOI: 10.1039/c3cp52894d

www.rsc.org/pccp

Siyuan Rao,<sup>a</sup> Zhibin Guo,<sup>a</sup> Dawei Liang,<sup>ab</sup> Deliang Chen,<sup>\*c</sup> Yen Wei<sup>d</sup> and Yan Xiang<sup>\*ab</sup>

The biohybrid sensor is an emerging technique for multi-functional detection that utilizes the instinctive responses or interactions of biomolecules. We develop a biohybrid pH sensor by taking advantage of the pH-dependent photoelectric characteristics of proteorhodopsin (pR). The transient absorption kinetics study indicates that the photoelectric behavior of pR is attributed to the varying lifetime of the M intermediate at different environmental pH values. This pR-based biohybrid light-powering sensor with microfluidic design can achieve real-time pH detection with quick response and high sensitivity. The results of this work would shed light on pR and its potential applications.

The rhodopsin class protein inherently possesses unique photophysical properties and is believed to be a candidate for photoelectric applications.<sup>1,2</sup> For instance, bacteriorhodopsin (bR), a membrane protein extracted from *Halobacterium salinarum* with a light-driven proton pump function, has great potential when applied in photochromic and photoelectronic devices.<sup>3–5</sup> Sharing the same structure, chromophore, and light-driven proton pump function with bR,<sup>6</sup> proteorhodopsin (pR) is a photoactive membrane protein derived from *Proteobacteria*,<sup>7</sup> and exhibits many photophysical characteristics that are similar to bR.<sup>8–10</sup> Unlike bR, whose stability is greatly dependent on its own trimer structure and hexagonal crystalline lattice in the sub-micro scale purple membrane,<sup>3</sup> the pR monomer is stable in detergent and phospholipid environments;<sup>11,12</sup> such stability is beneficial in the reconstitution of pR into pR–phospholipid bilayers as photoactive

monomers on the nanoscale. The large amount of pR protein that is quickly achieved through genetic engineering makes pR highly applicable to photoelectric devices.<sup>13</sup>

Discovered in the last decade, pR is believed to have a significant impact on energy flux in marine systems.<sup>14–17</sup> Upon illumination, pR undergoes a photocycle and “pumps” proton from the cytoplasmic to the extracellular medium, thus creating an electrochemical potential across the membrane. This electrochemical potential in turn promotes ATP synthesis. Most studies on pR are focused on its ecological distribution,<sup>18,19</sup> protein structure resolution,<sup>20,21</sup> and proton transfer mechanism.<sup>22,23</sup> Therefore, research on the photoelectric conversion of pR and its application remains limited. In biophysics and biochemistry, pR possesses pH-dependent proton transport efficiency.<sup>8,22,24,25</sup> The Kamo group was the first to propose a method to measure a quick pH change in photo-induced pR proton transfer using a SnO<sub>2</sub> transparent electrode.<sup>26</sup> However, the application of pR, particularly its pH-dependent property, as basal material in developing a device to monitor environmental pH has yet to be established.

In the present work, we successfully developed a pR-based biohybrid photoelectric device by assembling pR on an indium tin oxide (ITO) electrode (Fig. 1a) and achieved distinct photocurrent signals. This pR-based biohybrid photoelectric device exhibits noticeably sensitive responses to pH variation. Integrated with microfluidic design, the pR-based biohybrid pH sensor developed in this study can monitor environmental pH in real time with quick response and high sensitivity.

pR was obtained through protein expression and purification, following the protocol described in Fig. S1.† To protect protein activity, pR was embedded into phosphatidylcholine (PC; hereafter referred to as reconstituted pR, with pR:PC in a 1:50 molar ratio) as in a biomimetic environment. A reconstituted pR layer was then constructed on the surface of the ITO electrode to form a biohybrid device through the evaporation-induced assembly (Fig. S1–S3†). The field effect scanning electron microscopy (SEM) profiles demonstrate that the working area of the ITO glass electrode is homogeneously covered with

<sup>a</sup> Key Laboratory of Bio-Inspired Smart Interfacial Science and Technology of Ministry of Education, School of Chemistry and Environment, Beihang University, Beijing, 100191, P.R. China

<sup>b</sup> Beijing Key Laboratory of Bio-inspired Energy Materials and Devices, Beihang University, Beijing, 100191, P. R. China. E-mail: xiangy@buaa.edu.cn; Fax: +86-010-82339539; Tel: +86-010-82339539

<sup>c</sup> College of Life Science, Graduate University, Chinese Academy of Sciences, Beijing 100049, P. R. China. E-mail: dlchen@ucas.ac.cn; Tel: +86-010-88256585

<sup>d</sup> Department of Chemistry, Tsinghua University, Beijing, China

† Electronic supplementary information (ESI) available. See DOI: 10.1039/c3cp52894d

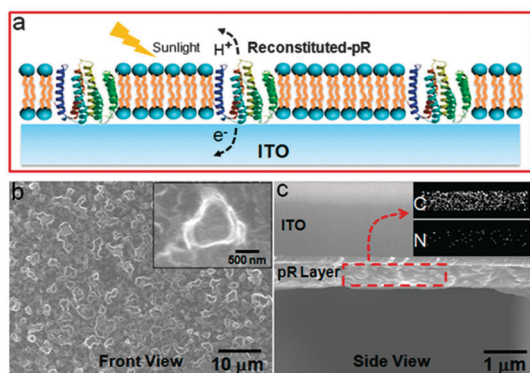


**Fig. 1** Design scheme of the pR-based biohybrid photoelectric device and the morphology of the reconstituted-pR deposition layer on the ITO electrode. (a) The pR protein embedded into phosphatidylcholine is immobilized onto the surface of the ITO electrode to form a pR-based biohybrid photoelectric device. (b and c) SEM and EDX images of the reconstituted pR layer. The reconstituted pR is well deposited and evenly distributed on the ITO electrode. The element distribution of carbon and nitrogen in the inset reveals the organic components in the reconstituted pR deposition layer.

reconstituted pR (Fig. 1b and c). The carbon and nitrogen elements examined by SEM and energy dispersive X-ray spectroscopy (EDX) in the inset of Fig. 1c further prove the uniform distribution of the reconstituted pR on the electrode surface.

A typical photoelectric response characterized by a prompt spike-like photocurrent was successfully achieved in the prepared pR-based photoelectric device (Fig. 2a) in a custom-designed photoelectric measuring system (Fig. S4†) by introducing flickering light with light-on and light-off stimulation. A photoelectric signal was not apparent with the ITO electrode deposited only with PC (Fig. S5†). The effects of pR concentration and light intensity were investigated to understand the factors that regulate photocurrent generation in the pR-based photoelectric device. A good linear relationship between pR concentration and photocurrent intensity was found (Fig. 2b). That is, photocurrent was enhanced from approximately  $5.0 \text{ nA cm}^{-2}$  to  $30.0 \text{ nA cm}^{-2}$  in proportion to the pR concentration ranging from  $0.1 \text{ mg mL}^{-1}$  to  $0.8 \text{ mg mL}^{-1}$  (protein concentration of reconstituted pR solution before deposition), as shown in Fig. S6–S7.† A similar effect of light intensity on photocurrent generation was also observed. The photocurrent was found to be positively proportional to the light intensity (Fig. 2c, Fig. S8†). The regulation of photocurrent provides a flexible method for further investigation.

The effects of environmental pH on photocurrent generation in the pR-based device were investigated with fixed protein concentration ( $0.8 \text{ mg mL}^{-1}$ ) and light intensity ( $318 \text{ mW cm}^{-2}$ ). With the pH changing from 4 to 10, the photocurrent density of the pR-based device presents a sigmoid curve, and high photocurrent density can be achieved under alkaline conditions (Fig. 3a). This device was found to be sensitive to pH ranging from 6 to 8.

Photocurrent generation generally reflects the process of proton transfer in the pR protein. According to the pR photocycle mechanism, the pR protein goes through a series of photochemical reactions and forms diverse intermediates once

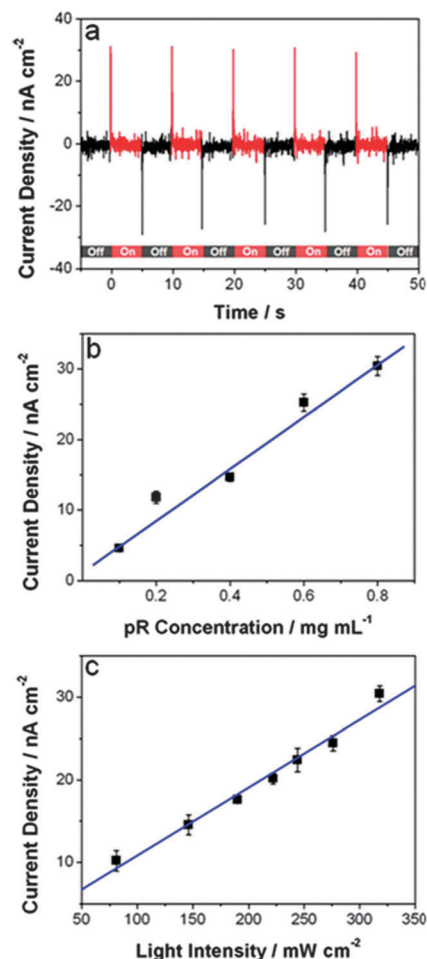


**Fig. 2** Typical photocurrent generation and its regulation by pR concentration and light intensity. (a) Spike-like and prompt photocurrent was generated upon flickering light stimulation. About  $30 \text{ nA cm}^{-2}$  photocurrent was achieved with  $0.8 \text{ mg mL}^{-1}$  of pR protein concentration and  $318 \text{ mW cm}^{-2}$  light intensity. (b) The relationship between pR concentration and photocurrent density. The photocurrent density steadily increases in proportion to the pR concentration in the range of  $0.1 \text{ mg mL}^{-1}$  to  $0.8 \text{ mg mL}^{-1}$  upon illumination with a light intensity of  $318 \text{ mW cm}^{-2}$ . (c) A linear relationship between light intensity and photocurrent was obtained when the pR-based device was illuminated with a light intensity ranging from  $81 \text{ mW cm}^{-2}$  to  $318 \text{ mW cm}^{-2}$ .

light drives the pR proton pump.<sup>10,24</sup> Among all the photochemical intermediates, the M intermediate is the most crucial in the proton transfer process;<sup>9,22,24</sup> furthermore, the lifetime of the M intermediate is considered essential for proton pump efficiency.<sup>2</sup> Through the transient absorption kinetics study, the M intermediate was found to display a long lifetime in an alkaline environment. High M intermediate accumulation promotes the proton pump efficiency of pR and results in the enhancement of the proposed device. The relationship between the lifetime of the M intermediate and pH is similar to that of the photocurrent and pH (Fig. 3a). The curve slope of the lifetime of the M intermediate implies that the  $\text{pK}_a$  of the proton release complex for pR is around 7.3 (Fig. S9†), thus suggesting a favorable accumulation in an alkaline environment. However, the K or O intermediate does not display any

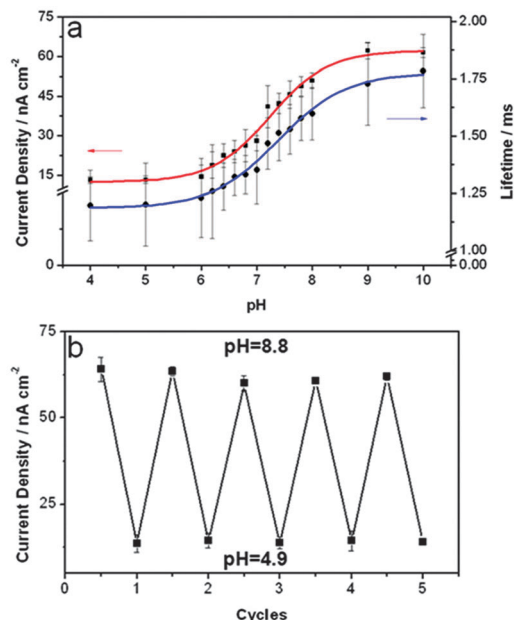


**Fig. 3** Photocurrent generation regulated by environmental pH and the reversibility of the photocurrent under an alternating pH environment. (a) The photocurrent generated by the pR-based photoelectric device exhibits a sigmoid curve when the environmental pH changes from 4 to 10 (red line). The photocurrent shows high sensitivity in the pH range of 6 to 8. The lifetime of the M intermediate, which is the most important photocycle intermediate that contributes to the proton pump function of pR, also varies with the changing environmental pH (blue line) within a millisecond scale. The behavior of the M intermediate lifetime, which varies with the pH, is closely related to that of the photocurrent generation. (b) The photocurrent of the pR-based photoelectric device presents good reversibility under an alternating pH environment. After repeatedly altering the environmental pH between 4.9 and 8.8 several times, the photocurrent density remains reversible in either an acidic or alkaline environment.

distinct relationship with the pH (Fig. S10†). As the lifetime of the M intermediate is detected to be within milliseconds, the prompt photocurrent generation would allow the pR-based device to perform fast pH detection. Furthermore, reversible photocurrent could be repeatedly generated through the pR-based device with alternating pH (Fig. 3b). Good pH sensitivity and reversibility give the pR-based device great potential in the development of a sensitive and quick-responding pH sensor.<sup>27</sup>

A custom pR-based pH sensor with microfluidic design was developed to monitor the variation of environmental pH (Fig. S11†). When influents with pH 5.0, 7.0, and 9.0 were consecutively injected into the pR-based sensor in sequence, a steady pH-dependent photocurrent was detected (Fig. 4a); that is, about  $10 \text{ nA cm}^{-2}$  at pH 5.0,  $30 \text{ nA cm}^{-2}$  at pH 7.0 and  $60 \text{ nA cm}^{-2}$  at pH 9.0. The photocurrent performance under pH variation is consistent with the results shown in Fig. 3a. This pR-based pH sensor also possesses noticeable reversibility for the alternating pH.

Dynamic pH variation was successfully monitored in real time using the pR-based pH sensor. A photocurrent density of about  $30 \text{ nA cm}^{-2}$  was initially recorded when the pR-based sensor was continuously injected with a buffer solution with

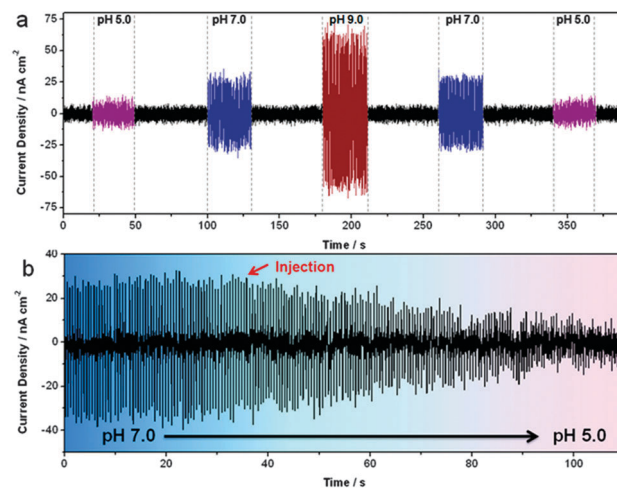


**Fig. 4** Real-time pH monitoring of dynamic pH variation with the pR-based biohybrid light-powering pH sensor. (a) Photocurrent of the pR-based pH sensor obtained during a continuous influent pH variation process. The black signals indicate the background current when the pR-based pH sensor is operated in the dark. Different photocurrent densities are detected based on the pH variation, that is, about  $10 \text{ nA cm}^{-2}$  for pH 5.0,  $30 \text{ nA cm}^{-2}$  for pH 7.0, and  $60 \text{ nA cm}^{-2}$  for pH 9.0. This result is consistent with the data achieved by the device operated in static state. The pR-based pH sensor maintains satisfactory photocurrent reversibility under alternating pH. (b) Photocurrent collected in the real-time monitoring of a dynamic and continuously varying pH using the pR-based biohybrid light-powering pH sensor. A clear photocurrent variation process is observed, with the aqueous solution pH changing from 7.0 to 5.0. Upon injection of another influent ( $50 \mu\text{L min}^{-1}$ ) with pH 5.0 into the chamber of the sensor, in which the initial pH of the buffer solution is 7.0, the photocurrent immediately declines and then gradually decreases from  $30 \text{ nA cm}^{-2}$  to about  $10 \text{ nA cm}^{-2}$  until the solution pH gradually reaches equilibrium at 5.0.

pH 7.0 (Fig. 4b). Once the injection solution was replaced by a pH 5.0 buffer, the photocurrent gradually decreased with a rate relevant to the injection flow rate. The result reflects the dynamic pH variation in the microfluidic flow. The decline of the photocurrent did not end until the pH of the buffer solution in the chamber reached equilibrium pH of 5.0.

Most biosensors are mainly based on fluorescence,<sup>28–30</sup> colorimetric,<sup>31–33</sup> or phosphorescence<sup>34</sup> outputs, all of which are time consuming and unsuitable for time-resolved environmental pH detection.<sup>35</sup> The novel pR-based biohybrid light-powering pH sensor proposed in the present study provides fast, sensitive and label-free pH detection by utilizing its instinctive photoelectric (electrochemical) signals. We believe this study could enlighten pR as a promising photoelectric biomaterial and provide a new avenue for the use of pR in biosensor applications.

## Acknowledgements

This work was financially supported by the National Major Fundamental Research Program of China (2011CB935700), the National Natural Science Foundation (U1137602, 21073010, 21103201, 51108014, 31070662, and 31170794), the Program for New Century Excellent Talents in University, the Specialized Research Fund for the Doctoral Program of Higher Education

of China (20111102120045), and the Fundamental Research Funds for the Central Universities. We thank Prof. J. D. Ding (Fudan University) and Prof. J. Zhai (Beihang University) for their beneficial discussions and equipment support.

## Notes and references

- 1 R. R. Birge, *Annu. Rev. Phys. Chem.*, 1990, **41**, 683–733.
- 2 T. Kikukawa, J. Tamogami, T. Shimono, M. Demura, T. Nara and N. Kamo, Photo-induced Proton Transfers of Microbial Rhodopsins, in *Molecular Photochemistry-Various Aspects*, ed. S. Saha, 2012.
- 3 N. A. Hampp, *Appl. Microbiol. Biotechnol.*, 2000, **53**, 633–639.
- 4 Y. D. Jin, T. Honig, I. Ron, N. Friedman, M. Sheves and D. Cahen, *Chem. Soc. Rev.*, 2008, **37**, 2422–2432.
- 5 N. K. Allam, C. W. Yen, R. D. Near and M. A. El-Sayed, *Energy Environ. Sci.*, 2011, **4**, 2909–2914.
- 6 J. M. Walter, D. Greenfield and J. Liphardt, *Curr. Opin. Biotechnol.*, 2010, **21**, 265–270.
- 7 O. Beja, *Science*, 2000, **289**, 1902–1906.
- 8 R. Krebs, U. Alexiev, R. Partha, A. DeVita and M. Braiman, *BMC Physiol.*, 2002, **2**, 5.
- 9 A. K. Dioumaev, J. M. Wang, Z. Balint, G. Varo and J. K. Lanyi, *Biochemistry*, 2003, **42**, 6582–6587.
- 10 G. Varo, L. S. Brown, M. Lakatos and J. K. Lanyi, *Biophys. J.*, 2003, **84**, 1202–1207.
- 11 M. J. Ranaghan, S. Shima, L. Ramos, D. S. Poulin, G. Whited, S. Rajasekaran, J. A. Stuart, A. D. Albert and R. R. Birge, *J. Phys. Chem. B*, 2010, **114**, 14064–14070.
- 12 M. J. Ranaghan, C. T. Schwall, N. N. Alder and R. R. Birge, *J. Am. Chem. Soc.*, 2011, **133**, 18318–18327.
- 13 H. J. Liang, G. Whited, C. Nguyen and G. D. Stucky, *Proc. Natl. Acad. Sci. U. S. A.*, 2007, **104**, 8212–8217.
- 14 O. Beja, E. N. Spudich, J. L. Spudich, M. Leclerc and E. F. DeLong, *Nature*, 2001, **411**, 786–789.
- 15 D. L. Man, W. W. Wang, G. Sabehi, L. Aravind, A. F. Post, R. Massana, E. N. Spudich, J. L. Spudich and O. Beja, *EMBO J.*, 2003, **22**, 1725–1731.
- 16 S. J. Giovannoni, L. Bibbs, J. C. Cho, M. D. Stapels, R. Desiderio, K. L. Vergin, M. S. Rappe, S. Laney, L. J. Wilhelm, H. J. Tripp, E. J. Mathur and D. F. Barofsky, *Nature*, 2005, **438**, 82–85.
- 17 E. F. DeLong and O. Béjà, *PLoS Biol.*, 2010, **8**, e1000359.
- 18 J. R. de la Torre, L. M. Christianson, O. Beja, M. T. Suzuki, D. M. Karl, J. Heidelberg and E. F. DeLong, *Proc. Natl. Acad. Sci. U. S. A.*, 2003, **100**, 12830–12835.
- 19 N. U. Frigaard, A. Martinez, T. J. Mincer and E. F. DeLong, *Nature*, 2006, **439**, 847–850.
- 20 Y. Furutani, D. Ikeda, M. Shibata and H. Kandori, *Chem. Phys.*, 2006, **324**, 705–708.
- 21 G. Schafer, S. Shastri, M. K. Verhoeven, V. Vogel, C. Glaubitz, J. Wachtveitl and W. Mantele, *Photochem. Photobiol.*, 2009, **85**, 529–534.
- 22 T. Friedrich, S. Geibel, R. Kalmbach, I. Chizhov, K. Ataka, J. Heberle, M. Engelhard and E. Bamberg, *J. Mol. Biol.*, 2002, **321**, 821–838.
- 23 E. Lorinczi, M. K. Verhoeven, J. Wachtveitl, A. C. Woerner, C. Glaubitz, M. Engelhard, E. Bamberg and T. Friedrich, *J. Mol. Biol.*, 2009, **393**, 320–341.
- 24 A. K. Dioumaev, L. S. Brown, J. Shih, E. N. Spudich, J. L. Spudich and J. K. Lanyi, *Biochemistry*, 2002, **41**, 5348–5358.
- 25 M. Lakatos, J. K. Lanyi, J. Szakács and G. Váró, *Biophys. J.*, 2003, **84**, 3252–3256.
- 26 J. Tamogami, T. Kikukawa, S. Miyauchi, E. Muneyuki and N. Kamo, *Photochem. Photobiol.*, 2009, **85**, 578–589.
- 27 S. Xu, Y. Qin, C. Xu, Y. Wei, R. Yang and Z. L. Wang, *Nat. Nanotechnol.*, 2010, **5**, 366–373.
- 28 E. M. Cornett, E. A. Campbell, G. Gulenay, E. Peterson, N. Bhaskar and D. M. Kolpashchikov, *Angew. Chem., Int. Ed.*, 2012, **51**, 9075–9077.
- 29 X. Zhang, S. Rehm, M. M. Safont-Sempere and F. Würthner, *Nat. Chem.*, 2009, **1**, 623–629.
- 30 H. Zhu, J. Fan, Q. Xu, H. Li, J. Wang, P. Gao and X. Peng, *Chem. Commun.*, 2012, **48**, 11766–11768.
- 31 S. Bi, Y. Yan, S. Hao and S. Zhang, *Angew. Chem., Int. Ed.*, 2010, **49**, 4438–4442.
- 32 D. Wencel, B. MacCraith and C. McDonagh, *Sens. Actuators, B*, 2009, **139**, 208–213.
- 33 L. N. Sun, H. Peng, M. I. J. Stich, D. Achatz and O. S. Wolfbeis, *Chem. Commun.*, 2009, 5000–5002.
- 34 Y. Liu, M. Li, Q. Zhao, H. Wu, K. Huang and F. Li, *Inorg. Chem.*, 2011, **50**, 5969–5977.
- 35 Y. Jia, R. Duan, F. Hong, B. Wang, N. Liu and F. Xia, *Soft Matter*, 2013, **9**, 6571–6577.